Nanoscale

Accepted Manuscript

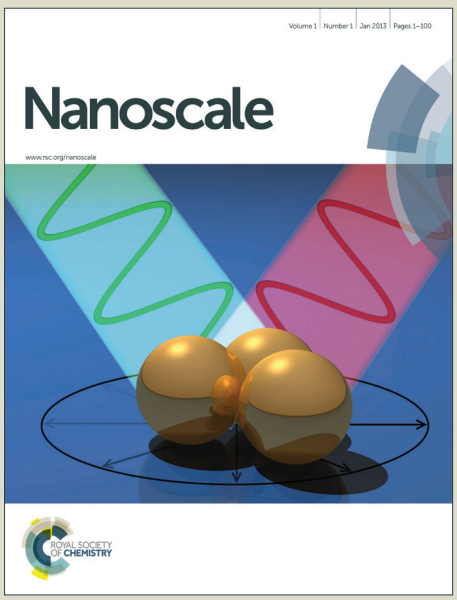

ROYAL SOCIETY OF CHEMISTRY

www.rsc.org/nanoscale

Journal Name

RSCPublishing

COMMUNICATION

Tunable Optical Activity of Plasmonic Dimers Assembled by DNA Origami

Cite this: DOI: 10.1039/x0xx00000x

Chengcheng Rao [a], Zheng-Gang Wang [b], Na Li [b], Wei Zhang[c*], Xuecheng Xu [a*] and Baoquan Ding [b*]

Received 00th January 2012,
Accepted 00th January 2012

DOI: 10.1039/x0xx00000x

www.rsc.org/

We investigate the optical response of gold nanorod (AuNR) dimers assembled in parallel on DNA origami template. Plasmonic circular dichroism (CD) was found to be highly dependent on the orientation of the dimers relative to DNA axis and the inter-rod distances. Dipole-dipole distances play a critical role in the induced plasmonic chirality. The orientation dependence of induced CD was further verified by AuNR/Au nanosphere (AuNS) heterodimers. The experimental results of the plasmonic CD agreed well with theoretical calculations.

Chiral nanocrystals and nanostructures have attracted considerable attention in recent decades[1-5]. However, the synthesis of artificial chiral nanomaterials, in the aspect of the structural and handedness control, is still time-consuming and costly. In comparison, self-assembly is considered as an efficient method to enable the fabrication of three-dimensional chiral superstructures with a variety of geometries, such as tetrahedral[6] and helical[7-9] configurations, which mimicked the natural chiral molecules. More than four nanoscale components are usually required to construct the 3D asymmetrical geometries. Assembly of 3D chiral nanostructures with significant circular dichroism (CD) response and fewer nanoparticles still remains as the challenge, but it is of great significance in biomimicking and nanofabrication[10].

In 3D chiral nanostructures, the precise control of geometrical parameters, such as the spatial orientation, position of the nanoelements and inter-components separations, is critical for tuning CD signals. Structural DNA nanotechnology[11-17] has been demonstrated as a programmable methodology for bottom-up fabrication of complex nanostructures with well-defined shapes and well-controlled functionalities. In particular, DNA origami[18], which is featured with unprecedented flexibility and spatial addressability, makes a programmable breadboard for placement of a variety of nanoscale objects. DNA origami has been successfully used as the template for single-molecule chemical reactions[19], DNA motors[20] and biomolecular networks[21]. In addition, DNA origami template has been used for site-selectively immobilized metal[22] and semiconductor nanoparticles[23] with nanometer precision, aiming for optical nanoantenna[24], surface-enhanced Raman scattering and waveguides[25, 26]. Notably, the assembly of noble metals nanoparticles, such as gold[27-32] or silver[33], can be directed by DNA origami template to achieve geometrical regulation of the nanoparticles construction, resulting in the controllable models of interparticle plasmon resonance and tunable field-enhancement effects. An example can be found in the fabrication of centrally symmetric chains with progressively decreasing size and separations of six gold nanoparticles[34], which can theoretically enhance the local field by orders of magnitude. Previously spherical gold nanparticles in helical[35] or tetrameric[36] configurations have been successfully arranged with DNA origami template, and the spatial positions and the interparticles separations were strictly controlled. The asymmetric frame, integrating the dynamic Coulombic dipole−dipole and electromagnetic interactions, resulted in chiral response with controllable CD shape and intensity in the visible wavelength range, demonstrating the great potential of DNA origami in the construction of chiral artificial plasmonic nanostructures.

Distinctive from spherical nanoparticles, anisotropic metal nanoparticles, such as gold nanorods (AuNRs), possessed two orthogonal plasmon resonances, and two nanorods can interact with each other in an orientation-dependent manner. The anisotropy also allows the use of the minimum of two nanorods for the fabrication of the 3D mirrored asymmetric architectures. DNA origami was used as the template for self-assembly of discrete AuNRs dimers to achieve CD response, the intensity and the shape of which were efficiently regulated through adjusting the spatial configuration. On the other hand, the previous work[27, 30, 32] focused on the crossed orientation of AuNR dimers, and the hybridization of the plasmons was considered as the dominant role in the 3D chirality. However, it has to be noted that in the AuNRs/DNA complex systems, the double-stranded DNA (dsDNA) helices may also take part in the chiral response[37], because of the coulomb interactions between the chiral molecules and the plasmonic nanoparticles. With the bifacial DNA rectangular sheet the template, dsDNA helices are unidirectionally oriented along the long axis of the origami, and such anisotropic interaction may efficiently transfer the chirality from the chiral molecule to the plasmonic particle. The induced chirality was ever found in the individual AuNR assembled on DNA rectangular origami[30] and chiral cysteine/AuNRs assemblies[38]. Previous simulations reveal that the enhanced plasmonic CD signal is based on the Coulomb interaction between chiral molecules and nanosphere dimers[39], but little is known about the role of DNA helices-nanorods interactions in the chiral response on experimental and theoretical levels, while this is of great significance for understanding the origin of the chirality of the plasmonic anisotropic nanoparticles self-assemblies.

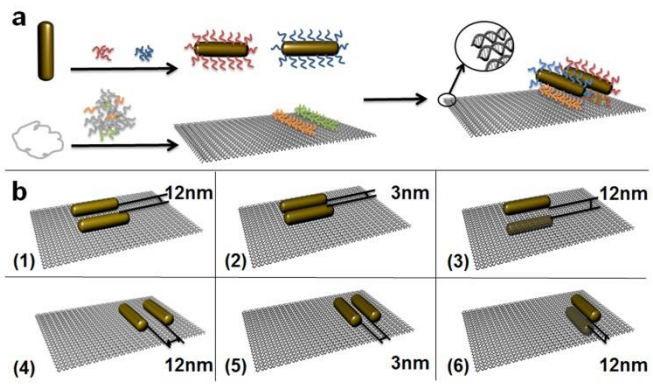

Figure 1 Schematic illustration of the DNA origami directed assembly of gold nanorod architectures. (a) DNA capture strands are extended from the surface of bifacial DNA origami template to form multiple binding sites. The binding sites with different DNA sequences are illustrated using different colors. AuNRs functionalized with corresponding complementary DNA strands are assembled at the predesignated locations on the origami template through DNA hybridization. (b) A series of AuNR dimers architectures were assembled by precisely tailoring the location of the capture strands on the origami template: (1, 2) two AuNRs assembled on the same side of template, parallel to the axis of the dsDNA helices (3) two AuNRs assembled on opposite side of template, parallel to the axis of the dsDNA helices; (4, 5) two AuNRs assembled on the same side of template, perpendicular to the axis of the dsDNA helices; (6) two AuNRs assembled on opposite side of template, perpendicular to the axis of the dsDNA helices. The distance between designed binding sites was estimated as the inter-rod distance.

Therefore, in this work, with DNA rectangular origami as the template we fabricated side-by-side AuNRs dimers, the geometric symmetry of which was significantly enhanced compared with the crossed configurations of nanorods as reported[27, 30, 40, 41]. The effect of the dimers orientations and the inter-rod distance on CD signals was investigated, and it was found that giant optical activity of AuNR dimers were induced by the oriented dsDNA helices through dipole-dipole interactions, which could be well described by the theoretical models (see Figure S5 in the support information). Our study may provide insight for the mechanism of the chirality in plasmonic architectures assembled by DNA nanostructures.

Figure 1a illustrates the experimental scheme. A rectangular DNA origami (90nm×60nm×2nm) was assembled by annealing the designed staple strands, capture strands and M13 scaffold DNA from 90^{o}C to room temperature for 14 hours (for the experimental details and sequence design, see Supporting Information). The product was then purified with a filter device (100kDa, molecular weight cutoff (MWCO), Amicon, Millipore) to remove the excessive staple and capture strands. DNA capture strands with carefully designed sequences (in orange and green) were extended from the rectangular DNA template at two specific sites to organize AuNRs precisely. The binding sites were located either on the same side or the opposite sides, and two binding sites were arranged in the side-by-side fashions. At each binding site, ten capture strands with identical-sequence were used to immobilize one AuNR (39nm×12nm). To avoid nonspecific binding, the capture sequences were different at the two individual binding sites. The purified DNA origami and AuNRs functionalized with corresponding complementary DNA strands were mixed and annealed from 43^{o}C to 23^{o}C for over 48h. After DNA hybridization, AuNRs were assembled at the designated binding sites on the DNA template to form side-by-side geometrical configurations. To thoroughly investigate the effect of DNA helices on the chirality of AuNR dimers, side-by-side AuNR dimers were arranged perpendicular or parallel to the long side of the rectangular origami sheet (*i.e.* the axis of the dsDNA helices), on one side or opposite sides, with different inter-rod distances. Single AuNR was also assembled onto the origami surface, perpendicular or parallel to the axis of dsDNA helices as the control, following similar experimental procedures.

The annealed products were analyzed by agarose gel electrophoresis, and the resulting gel image is shown in Supporting Information Figure S1. Lanes 3-8 correspond to AuNR dimeric structures (1)-(6) in Figure 1b. The target gel bands were then sliced and extracted by electro-elution with dialysis tube membranes (MWCO: 50K). Figure 2b show transmission electron microscopy (TEM) images of AuNR dimers that were arranged on same side and opposite sides of the origami surface, respectively. Figure 2a shows the TEM images of single AuNR on the origami. The stained structures of the products in TEM matched well with schematically

illustrated structural characters of the self-assemblies, including side-by-side geometrical dimer configurations, parallel and perpendicular orientation relative to the long side of the origami sheet. This demonstrates the precise control of AuNRs arrangement by the rectangular origami template. The inter-rod distance in TEM images is not exactly equal to the theoretical value estimated from the designed structures, which is attributed to the capillary force during the drying process on the TEM grids. More TEM images can be found in Figure S2.

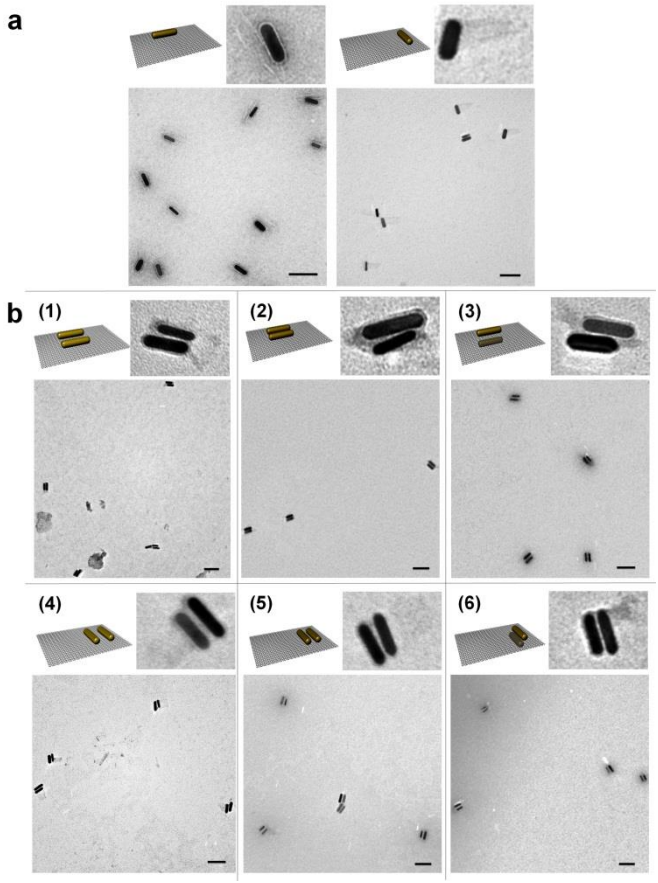

Figure 2 TEM images of AuNRs/origami nanostructures. (a) TEM images of control groups with only one AuNR assembled on the DNA origami. (b) TEM images of the designed nanostructures corresponding to Fig.1b (1)-(6). The scale bar in all above images is 100 nm.

CD measurements were carried out with a quartz cuvette using a J-810 Circular Dichroism Spectrometer. All the samples were dispersed in water-based 1×TAE/Mg^{2+} buffer. The CD spectra of the six side-by-side AuNR dimeric structures are shown in Figure 3a. It is evident that the plasmonic dimers perpendicular and parallel to dsDNA helices exhibit bisignate spectra bands with opposite chirality, characteristics of right-handed and left-handed self-assemblies. It was also found that the arrangement of side-by-side AuNR dimers on the opposite side of the origami sheet displayed larger CD response than on the same side. These results indicate that the dipole-dipole interactions between dsDNA helices and AuNRs may affect the chirality of the complex assemblies significantly. Moreover, AuNR dimers on the same side displayed stronger CD signals than single AuNR, and smaller inter-rod distance resulted in the larger chiral response. The dependence of the CD intensity on the rod number and spacing may reflect the cooperative dipole interactions between AuNR dimers and dsDNA helices.

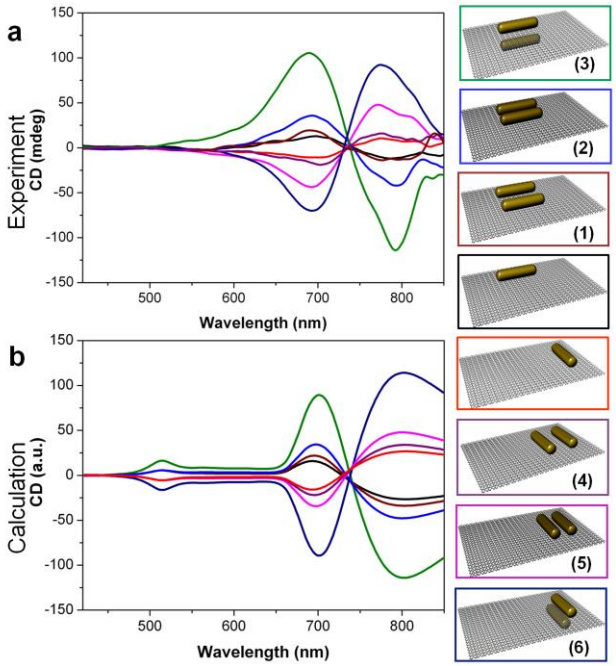

Figure 3 CD spectra of the AuNRs/origami nanostructures. (a) Experimental CD spectra of the designed nanostructures and control groups. The AuNR concentrations of all of the samples are the same. (b) Calculation results of the CD spectra. Each plot (left) was correlated to the frame of the respective sample (right) through colors.

We also designed and constructed an asymmetric heterodimer composed of one 15 nm Au nanosphere (AuNS) and one AuNR onto the rectangular origami sheet, to further demonstrate the role of DNA helices in the chirality of the plasmonic self-assemblies, with a similar assembly procedure(Figure 4c and S5). Figure 4 shows the schematic drawing, CD spectra and TEM of the assembled heterodimer. Four AuNS/AuNR dimer architectures were designed: (1) AuNS and AuNR on opposite side of template with AuNR parallel to the axis of the dsDNA helices (red curve, surface distance 12 nm); (2) AuNS and AuNR on the same side of template with AuNR parallel to the axis of the dsDNA helices (black curve, surface distance 3 nm); (3)AuNS and AuNR on the same side of template with AuNR perpendicular to the axis of the dsDNA helices (blue curve, surface distance 3 nm); (4) AuNS and AuNR on the opposite side of template with AuNR perpendicular to the axis of the dsDNA helices (purple curve, surface distance 12 nm). Experimental measured CD showed that the parallel and perpendicular orientation of the nanorod in the dimers, relative to the axis of dsDNA helices, resulted in the opposite chiral response, and the heterodimers on the opposite side of the origami surface displayed stronger CD signals than those on the same side.

Here we present a qualitative theory to understand the basic features of these experimental results. Single AuNR that was not assembled on the DNA origami does not show any chiral response. Therefore, unlike the chiral properties in other systems in which AuNR dimers were arranged in crossed fashions, the CD spectrum of the composite system of DNA

origami and side-by-side AuNR dimers comes from the induction of the aligned dsDNA helices. We apply the dipole approximation method to study the optical properties in the following[38].

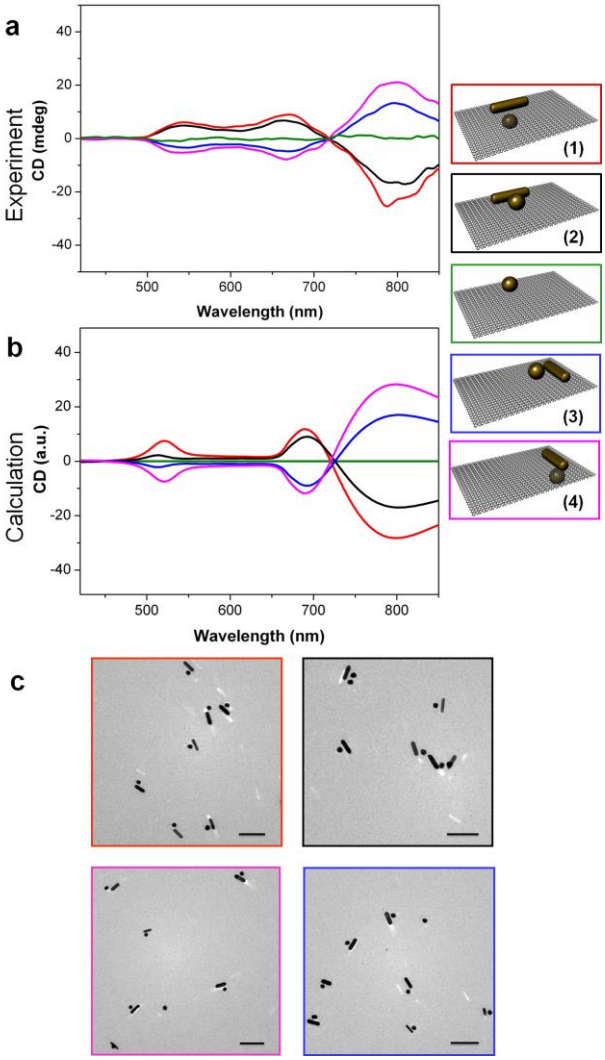

Figure 4 (a) Experimental CD spectra of the pre-designed AuNS-AuNR heterodimers nanostructures and control groups. The concentrations of all of the assembled heterodimers were the same. (b) The CD spectra of the assembled nanoarchitectures. Each plot (left) was correlated to the frame of the respective sample (right) through colors. (c) Corresponding TEM images AuNS-AuNR heterodimers. The scale bar in all above images is 100 nm.

A number of theoretical models proposed various possible mechanisms for plasmonic (or excitonic) CD induction[38,42,43]. In our approach, the AuNR/AuNS is represented by a dipole at its center, while the DNA origami may be viewed as effective dipole(s) at positions right opposite to the center of AuNR(s)/AuNS(s). The response of DNA origami/effective dipole(s) can be described by the polarizability tensor defined by $\vec{p}_D = \hat{\alpha} \cdot \vec{E}_D$, where $\vec{E}_D$ the electric field on the dipole(s) with moment $\vec{p}_D$. The electric field on the effective dipole of DNA origami is the summation of the incident field $\vec{E}_0$ and the dipole field from AuNR/AuNS

$$\frac{1}{R^3}[3\vec{n}(\vec{n}\cdot\vec{p}_M)-\vec{p}_M] \quad (1)$$

where R the distance between the effective dipoles (Figure S6), $\vec{n}$ the unit vector along the centers between the effective dipoles, the dipole of the AuNR $\vec{p}_M = \alpha_M \vec{E}_0$, α_M the effective polarizability of AuNR/AuNS. (See Support Information for more details) The dominant contribution of CD at visible light regime is the origami induced and AuNR/AuNS amplified absorption difference between left and right circularly polarized light, *i.e.*,

$$CD = Q_L - Q_R \quad (2)$$

$$Q_{L/R} = \mathrm{Im}(\alpha_M)\cdot\omega\cdot|\vec{E}^{L/R^*}\cdot\vec{E}^{L/R}|^2 \quad (3)$$

$$\vec{E}^{L/R} = \vec{E}_0^{L/R} + \frac{1}{R^3}[3\vec{n}(\vec{n}\cdot\vec{p}_D^{L/R}) - \vec{p}_D^{L/R}] \quad (4)$$

where $\vec{E}_0^{L/R}$ and $\vec{p}_D^{L/R}$ are the left/right circularly polarized incident field and the induce dipole of DNA origami in the presence of incident field. The corresponding theoretical results are shown in Figure 3b.

Impressively, the theoretical results are in good agreement with the experimental observations，and some important conclusions can be drawn from our theory. First, $CD \propto G_y$ ($CD \propto G_x$) (as seen in equation S9 in Support Information) is induced by chirality of DNA origami. Though $G_{x/y}$ is small in the visible light regime and the CD is hard to detect without AuNR/AuNS, the presence of AuNR/AuNS enhances the CD signal in the visible light regime due to the surface plasmon resonance (because $CD \propto \mathrm{Im}[\alpha_M]$). The anisotropic of DNA origami ($G_y = -G_x$) lead to opposite sign of CD for AuNR along X and Y directions. Moreover, the enhanced field on DNA origami due to multiple AuNR (for AuNR/AuNS dimer at the same side of DNA origami) or gap near field (for AuNR/AuNS dimer at the different sides of DNA origami) may further amplify the CD strength. The occurring of another CD signal is due to the plasmonic excitations along the transverse direction of AuNRs. The CD response at this wavelength is not obvious compared to the theoretical result. The main reason is that the inhomogeneous size distribution and imperfect shape of the synthesized AuNRs and relatively high CD signal of the longitudinal mode.

Conclusions

In summary, using rectangular DNA origami sheet as the template, side-by-side AuNRs dimers were fabricated. DNA-based assembly provided remarkable spatial control of plasmonic nanostructures and chiral molecules, which allow the unprecedented study of orientation dependence of chiral molecule-induced CD. CD response was largely affected by the dimers orientation relative to the axis of dsDNA helices and inter-rod distances. The experimental results are consistent with the theoretical simulation that took the dipoles of dsDNA helices into account, revealing the dominant role of dipole-dipole distances in the plasmonic chirality. The induction of the chirality from the plasmonic architectures by DNA helices were further verified by AuNS-AuNR heterodimers on the origami sheet. Our work may advance the development of the regulation methodologies and provide insights for the mechanisms of the chiral response of the plasmonic nanoparticles/chiral molecules complex.

Acknowledgements

This work was partially supported by the National Basic Research Program of China (973 Program, 2011CB922204), and the National Natural Science Foundations of China (21173059, 21222311, 11174042 and 11374039).

Notes and references

[a] Department of Physics, East China Normal University, No.500 Dong Chuan Road, 200241 Shanghai, China.
[b] Key Laboratory of Nanosystem and Hierarchical Fabrication, National Center for Nanoscience and Technology, Chinese Academy of Sciences, No. 11 BeiYiTiao, ZhongGuanCun, Beijing 100190, China.
[c] Institute of Applied Physics and Computational Mathematics, Beijing 100088, P. R. China
*Address correspondence to zhang_wei@iapcm.ac, xcxu@phy.ecnu.edu.cn and dingbq@nanoctr.cn

† Footnotes should appear here. These might include comments relevant to but not central to the matter under discussion, limited experimental and spectral data, and crystallographic data.
Electronic Supplementary Information (ESI) available: [details of any supplementary information available should be included here]. See DOI: 10.1039/c000000x/

1. N. J. Halas, S. Lal, W.-S. Chang, S. Link and P. Nordlander, *Chemical Reviews*, 2011, **111**, 3913-3961.
2. A. Guerrero-Martinez, B. Auguie, J. Lorenzo Alonso-Gomez, Z. Dzolic, S. Gomez-Grana, M. Zinic, M. Magdalena Cid and L. M. Liz-Marzan, *Angewandte Chemie-International Edition*, 2011, **50**, 5499-5503.
3. C. Gautier and T. Buergi, *Chemphyschem*, 2009, **10**, 483-492.
4. M. Hentschel, M. Schaeferling, T. Weiss, N. Liu and H. Giessen, *Nano letters*, 2012, **12**, 2542-2547.
5. D. E. Gomez, T. J. Davis and A. M. Funston, *Journal of Materials Chemistry C*, 2014.
6. W. Yan, L. Xu, C. Xu, W. Ma, H. Kuang, L. Wang and N. A. Kotov, *Journal of the American Chemical Society*, 2012, **134**, 15114-15121.
7. A. Kuzyk, R. Schreiber, Z. Fan, G. Pardatscher, E. M. Roller, A. Hogele, F. C. Simmel, A. O. Govorov and T. Liedl, *Nature*, 2012, **483**, 311-314.
8. R. Schreiber, N. Luong, Z. Fan, A. Kuzyk, P. C. Nickels, T. Zhang, D. M. Smith, B. Yurke, W. Kuang, A. O. Govorov and T. Liedl, *Nature communications*, 2013, **4**, 2948.
9. X. Lan, X. Lu, C. Shen, Y. Ke, W. Ni and Q. Wang, *Journal of the American Chemical Society*, 2015, **137**, 457-462.
10. S. Zeng, D. Baillargeat, H. P. Ho and K. T. Yong, *Chem Soc Rev*, 2014.
11. A. V. Pinheiro, D. R. Han, W. M. Shih and H. Yan, *Nature nanotechnology*, 2011, **6**, 763-772.
12. N. C. Seeman, *Nano letters*, 2010, **10**, 1971-1978.
13. T. Liedl, B. Hogberg, J. Tytell, D. E. Ingber and W. M. Shih, *Nature nanotechnology*, 2010, **5**, 520-524.
14. S. M. Douglas, H. Dietz, T. Liedl, B. Hogberg, F. Graf and W. M. Shih, *Nature*, 2009, **459**, 414-418.
15. A. Condon, *Nature Reviews Genetics*, 2006, **7**, 565-575.
16. Z. G. Wang and B. Q. Ding, *Advanced Materials*, 2013, **25**, 3905-3914.
17. Y. H. Roh, R. C. H. Ruiz, S. M. Peng, J. B. Lee and D. Luo, *Chemical Society Reviews*, 2011, **40**, 5730-5744.
18. P. W. K. Rothemund, *Nature*, 2006, **440**, 297-302.
19. N. V. Voigt, T. Torring, A. Rotaru, M. F. Jacobsen, J. B. Ravnsbaek, R. Subramani, W. Mamdouh, J. Kjems, A. Mokhir, F. Besenbacher and K. V. Gothelf, *Nature nanotechnology*, 2010, **5**, 200-203.
20. K. Lund, A. J. Manzo, N. Dabby, N. Michelotti, A. Johnson-Buck, J. Nangreave, S. Taylor, R. J. Pei, M. N. Stojanovic, N. G. Walter, E. Winfree and H. Yan, *Nature*, 2010, **465**, 206-210.
21. J. L. Fu, M. H. Liu, Y. Liu and H. Yan, *Accounts of Chemical Research*, 2012, **45**, 1215-1226.
22. Q. Liu, C. Song, Z. G. Wang, N. Li and B. Q. Ding, *Methods*, 2014, **67**, 205-214.
23. K. Du, S. H. Ko, G. M. Gallatin, H. P. Yoon, J. A. Liddle and A. J. Berglund, *Chemical communications*, 2013, **49**, 907-909.
24. A. P. Eskelinen, R. J. Moerland, M. A. Kostiainen and P. Torma, *Small*, 2014, **10**, 1057-1062.
25. D. K. Lim, K. S. Jeon, J. H. Hwang, H. Kim, S. Kwon, Y. D. Suh and J. M. Nam, *Nature nanotechnology*, 2011, **6**, 452-460.
26. M. Pilo-Pais, A. Watson, S. Demers, T. H. LaBean and G. Finkelstein, *Nano letters*, 2014, **14**, 2099-2104.
27. X. Lan, Z. Chen, G. Dai, X. Lu, W. Ni and Q. Wang, *Journal of the American Chemical Society*, 2013, **135**, 11441-11444.
28. S. Pal, Z. Deng, H. Wang, S. Zou, Y. Liu and H. Yan, *Journal of the American Chemical Society*, 2011, **133**, 17606-17609.
29. B. Q. Ding, Z. T. Deng, H. Yan, S. Cabrini, R. N. Zuckermann and J. Bokor, *Journal of the American Chemical Society*, 2010, **132**, 3248-3249.
30. X. Shen, P. Zhan, A. Kuzyk, Q. Liu, A. Asenjo-Garcia, H. Zhang, F. J. Garcia de Abajo, A. Govorov, B. Ding and N. Liu, *Nanoscale*, 2014, **6**, 2077-2081.
31. B. Ding, H. Wu, W. Xu, Z. Zhao, Y. Liu, H. Yu and H. Yan, *Nano letters*, 2010, **10**, 5065-5069.
32. A. Kuzyk, R. Schreiber, H. Zhang, A. O. Govorov, T. Liedl and N. Liu, *Nature Materials*, 2014, **13**, 862-866.
33. S. Pal, Z. T. Deng, B. Q. Ding, H. Yan and Y. Liu, *Angewandte Chemie-International Edition*, 2010, **49**, 2700-2704.
34. B. Ding, Z. Deng, H. Yan, S. Cabrini, R. N. Zuckermann and J. Bokor, *Journal of the American Chemical Society*, 2010, **132**, 3248-3249.
35. X. B. Shen, C. Song, J. Y. Wang, D. W. Shi, Z. A. Wang, N. Liu and B. Q. Ding, *Journal of the American Chemical Society*, 2012, **134**, 146-149.
36. X. Shen, A. Asenjo-Garcia, Q. Liu, Q. Jiang, F. J. Garcia de Abajo, N. Liu and B. Ding, *Nano letters*, 2013, **13**, 2128-2133.
37. V. A. Gerard, Y. K. Gun'ko, E. Defrancq and A. O. Govorov, *Chemical communications*, 2011, **47**, 7383-7385.
38. B. Han, Z. Zhu, Z. Li, W. Zhang and Z. Tang, *Journal of the American Chemical Society*, 2014.
39. H. Zhang and A. O. Govorov, *Physical Review B*, 2013, **87**.
40. W. Ma, H. Kuang, L. Xu, L. Ding, C. Xu, L. Wang and N. A. Kotov, *Nature communications*, 2013, **4**, 2689.
41. W. Ma, H. Kuang, L. Wang, L. Xu, W. S. Chang, H. Zhang, M. Sun, Y. Zhu, Y. Zhao, L. Liu, C. Xu, S. Link and N. A. Kotov, *Scientific reports*, 2013, **3**, 1934.
42. B. M. Maoz, Y. Chaikin, A. B. Tesler, O. Bar Elli, Z. Fan, A. O. Govorov and G. Markovich, *Nano letters*, 2013, **13**, 1203-1209.

43. A. O. Govorov, Z. Fan, P. Hernandez, J. M. Slocik and R. R. Naik, *Nano letters*, 2010, **10**, 1374-1382.

